Cation distribution in partially ordered columbite from the Kings Mountain pegmatite, North Carolina

Marc Wenger, Thomas Armbruster

Laboratorium für chemische und mineralogische Kristallographie, Universität Bern, Freiestrasse 3, CH-3012 Bern, Switzerland

Charles A. Geiger

Bayerisches Forschungsinstitut für experimentelle Geochemie und Geophysik, Universität Bayreuth, Postfach 101251, D-8580 Bayreuth, Germany

Abstract

Two columbite samples, space group *Pbcn,* with $a = 14.233$, $b = 5.724$, $c = 5.104$ Å, $Z = 4$ and $a = 14.221$, $b = 5.727$, $c = 5.102$ Å, of similar chemistry (average composition $Fe_{0.65}Mn_{0.30}Ti_{0.05}Nb_{1.5}Ta_{0.5}O_6$) but from different rock types of the Kings Mountain pegmatite, North Carolina, were investigated. One columbite specimen (NCP5) originates from a primary spodumene pegmatite, the other (NCP1) from a rock composed mainly of sugary albite formed by subsequent hydrothermal activity. Single-crystal X-ray structure refinements indicate that both columbite samples show strong disorder between (Nb,Ta) and (Fe,Mn) on octahedral A and B positions. This is in agreement with a Mössbauer spectrum (NCP5), which was fitted with two doublets characteristic of two distinct $^{[6]}Fe^{2+}$ sites. Both samples show strong chemical zoning with respect to Nb and Ta, but weak zoning of Fe and Mn. The similar chemical composition and cation ordering indicate that columbite in both rocks is formed by the same process. Late hydrothermal alteration of the original spodumene pegmatite did not affect the composition of the earlier crystallized columbite. The primary columbite (NCP5) shows slightly stronger disorder of two- and five-valent cations than columbite (NCP1) found in the hydrothermally altered part of the pegmatite.

Introduction

Minerals of the columbite-tantalite group have the general formula AB_2O_6, where typically $A = Fe^{2+}, Mn^{2+}$, Mg and $B = Nb^{5+}, Ta^{5+}$, with minor substitutions of Sn^{4+}, W^{6+}, and Fe^{3+}; they have space group *Pbcn* with $a = 14.3$, $b = 5.7$, $c = 5.1$ Å, $Z = 4$. The group comprises the end-members ferrocolumbite ($FeNb_2O_6$), manganocolumbite ($MnNb_2O_6$), manganotantalite ($MnTa_2O_6$), and magnocolumbite ($MgNb_2O_6$). The structures of these minerals can be interpreted as ordered superstructures of the brookite (TiO_2) or α-PbO_2 structure with 2 $(Nb,Ta)^{5+}$ + 1 $(Fe,Mn,Mg)^{2+} \rightleftharpoons 3$ Ti^{4+}. In contrast, $FeTa_2O_6$ belongs to the tetragonal tapiolite series, which has a structure related to that of rutile. Ixiolite and wodginite (Ferguson et al., 1976) are also related to columbite as they have a corresponding O arrangement with the same occupied octahedral sites but a different ordering pattern of A and B cations.

Ixiolite $(Ta^{5+}, Fe^{2+}, Sn^{4+}, Nb^{5+}, Mn^{2+})O_2 = \frac{1}{3} \cdot AB_2O_6$ was first described by Nordenskiöld (1857). Nickel et al. (1963a, 1963b) determined that the ixiolite structure is the columbite substructure (space group *Pbcn*, $a = 4.74$, $b = 5.73$, $c = 5.16$ Å, $Z = 4$) with a random distribution of A and B cations. Heating experiments on ixiolite cause a change in the X-ray powder diffraction pattern such that some samples reveal a wodginite pattern (Khvostova and Maximova, 1969), whereas others yield a columbite pattern (Nickel et al., 1963b). Only the first group includes "true" ixiolite; members of the second group are cation-disordered columbite and are called "pseudo-ixiolite" (Nickel et al., 1963b). The groups can also be distinguished on the basis of their chemical composition. True ixiolite contains more Sn^{4+}, Ti^{4+}, and Fe^{3+} than pseudo-ixiolite (Nickel et al., 1963a, 1963b). This chemical difference seems to be largely responsible for the different structural changes upon heating.

The crystal structure of columbite was solved by Sturdivant (1930). Relations between the unit cells of ixiolite, tantalite, and wodginite were investigated by Grice et al. (1976) and Ferguson et al. (1976). The latter authors adopted the idea of Laves et al. (1963) and Nickel et al. (1963b) to utilize the cell of ixiolite (which is similar to that of α-PbO_2) as a prototype for the three closely related structures. In this model, the cells of columbite and wodginite can be regarded as different supercells of ixiolite. Neutron-powder diffraction studies on several synthetic end-members with the columbite structure were described by Weitzel (1976). The structure of heat-treated natural manganotantalite has been refined from X-ray single-crystal data by Grice et al. (1976).

Cation ordering in natural columbite has been studied

as a function of changes in cell dimensions (e.g., Turnock, 1966; Wise et al., 1985). Komkov (1970) introduced the a/c ratio as an order-disorder parameter that was subsequently adopted by Černý and Turnock (1971). Using the available data, Ercit (1986) derived the following equation to estimate the degree of cation order for columbite in the $(Fe,Mn)(Nb,Ta)_2O_6$ system:

$$\% \text{ order } (\pm 5\%) = 1727 - 941.6 \times y,$$

where $y = c - 0.2329 \times a$. In agreement with observations on natural samples, electrostatic energy calculations (Giese, 1975) indicate that various cation ordering schemes within octahedral sites of the columbite structure lead to similar lattice energies. The most recent review of oxide minerals of Nb and Ta is given by Černý and Ercit (1989).

SAMPLE DESCRIPTION

The investigated samples originate from the Kings Mountain spodumene pegmatite district in North Carolina (Horton and Butler, 1986). The pegmatites are probably related to the neighboring Cherryville Granite and are of Mississippian age. A Rb-Sr whole rock age of the pegmatite was determined at 340 ± 5 m.y. (Kish, 1983). Within the Kings Mountain area, two pegmatite mining operations are presently active: the Foote mine (Kesler, 1961) and the FMC-Lithco Hallman-Beam mine (Spanjers, 1988). The minerals of the Foote mine were studied by White (1981), who distinguished several stages of crystallization. The primary stage produced a homogeneous (unzoned) pegmatite with microcline, quartz, and spodumene as the dominant phases. After the crystallization of these primary minerals, the pegmatite was squeezed into surrounding amphibolite and schist, both along and across foliation (White, 1981). Following the primary emplacement, characteristic longitudinal fractures and faults were developed allowing hydrothermal solutions in a secondary stage to circulate. These fluids partially dissolved spodumene, manganese apatite, beryl, microcline, and cassiterite, and the resulting rock became vuggy and devoid of spodumene. Microcrystalline quartz and albite are presently the major minerals filling the vugs. Li-rich solutions reacted with the wall rock forming the lithium amphibole holmquistite and Rb,Cs-rich biotite together with schorl, pyrrhotite, grossular, spessartine, ferroaxinite, and epidote-clinozoisite at the contact (White, 1981). The formation of this dense reaction zone at the wall rock trapped metal-rich solutions within the pegmatite. Upon cooling, these hydrothermal solutions produced tertiary stage phosphates, zeolites, and clay-serpentine minerals.

During a visit to the Lithco Hallman-Beam spodumene pegmatite mine in 1988, three characteristic Li-bearing samples (NCP1, NCP4, and NCP5) containing columbite were collected. The first sample (NCP5) came from large boulders of only slightly deformed pegmatite containing large megacrysts of spodumene (up to 30 cm in length), microcline, and booklets of muscovite within a medium-grained groundmass of quartz, albite, muscovite, and ac-

cessory columbite. This rock type is characteristic of the primary pegmatite. The columbite crystals (about 2 cm in their maximum dimension) are black, platy, and subhedral in habit with good cleavage parallel to {100}. The second rock type (NCP4) possesses the same minerals but is a brecciated product of type 1 (NCP5). Only fragments of greenish spodumene (less than 5 cm in their maximum dimension) are seen in a finer grained groundmass containing scattered columbite fragments (less than 1 mm in dimension). The third type (NCP1) is a dense, fine crystalline rock composed of approximately 90% sugary albite (crystal size: 0.1–0.3 mm) with some quartz. This rock has greenish spots that resemble the spodumene of the second rock type (NCP4). Thin section examination and electron microprobe analyses show that the green spots are reaction halos of orange-brown vug fillings containing mainly lithiophilite and clay minerals. Fine flakes of muscovite and splinters of columbite (up to 0.2 mm in dimension) are dispersed within the albite matrix. Sample NCP1 was certainly formed as a result of late hydrothermal activity and must be assigned to the secondary and tertiary stage of crystallization as defined by White (1981).

The present study was undertaken to determine the degree of cation order present in columbite of the primary rock (NCP5) and in the hydrothermal reaction product (NCP1).

EXPERIMENTAL PROCEDURES

Electron microprobe analyses

Electron microprobe analyses were carried out on both specimens using a wavelength dispersive (WDS) microprobe system (Cameca SX50). An accelerating potential of 15 kV, a beam current of 30 nA, and a beam size of approximately 1 μm were used. The following synthetic standards were used: $KNbO_3$ ($NbL\alpha$), $KTaO_3$ ($TaL\alpha$), $FeTiO_3$ ($FeK\alpha$, $TiK\alpha$), and $MnTiO_3$ ($MnK\alpha$). Natural cassiterite ($SnL\alpha$) and wollastonite ($CaK\alpha$) as well as pure W ($WL\alpha$) and Sb ($SbL\alpha$) provided reference intensities. The counting time was 30 s for Nb and Ta and 10 s for the remaining elements. No significant concentrations of Sb were detected. The raw data were corrected on-line for drift, deadtime, and background using PAP correction programs. The analyses and the formulas calculated on the basis of six O atoms are given in Table 1.

X-ray data measurements and refinement of columbite

Two columbite crystal fragments (crystal size 190 × 130 × 150 μm for sample NCP5 and 50 × 150 × 100 μm for sample NCP1) were examined with a precession camera to confirm their $Pbcn$ space group. Significant but weak intensity was found for the 200 reflection, indicating a low degree of cation order for both samples. Thus the crystals must be classified as poorly ordered columbite. To reduce effects related to thermal motion, intensity data of NCP5 were obtained at 100 K. (Unfortunately, the crystal was lost after the experiment.) Reflection

TABLE 1. Average electron microprobe analyses and formulas of columbite samples from the Kings Mountain district, North Carolina

Oxide	Wt%	Range	Standard deviation*	Cations	
Sample NCP5 based on eight analyses					
Nb_2O_5	50.53	49.80–51.25	0.61	Nb	1.46
Ta_2O_5	28.01	26.97–29.17	0.75	Ta	0.49
TiO_2	1.45	1.40–1.56	0.05	Ti	0.07
SnO_2	0.55	0.50–0.58	0.03	Sn	0.01
CaO	0.00	0	0.00	Ca	0.00
MnO	6.21	5.81–7.01	0.35	Mn	0.34
FeO	11.92	10.84–12.44	0.49	Fe	0.64
WO_3	0.13	0.00–0.34	0.13	W	0.00
Total	98.80				3.01
Sample NCP1 based on ten analyses					
Nb_2O_5	51.72	27.69–62.25	12.11	Nb	1.50
Ta_2O_5	28.68	18.54–49.75	10.99	Ta	0.50
TiO_2	1.30	0.50–3.41	0.97	Ti	0.06
SnO_2	0.46	0.00–2.25	0.67	Sn	0.01
CaO	0.01	0.00–0.04	0.02	Ca	0.00
MnO	5.34	4.31–5.76	0.51	Mn	0.28
FeO	13.03	11.47–14.06	0.83	Fe	0.68
WO_3	0.28	0.00–0.56	0.21	W	0.01
Total	100.82				3.04

Note: Analyses are normalized to six O atoms.
* Standard deviations are not derived from counting statistics but represent measured standard deviations for the statistical sampling which contributed to the average.

TABLE 2. Details of X-ray data measurement

	NCP5	NCP1
Temperature	100 K	293 K
a (Å)	14.189(6)	14.221(2)
b (Å)	5.727(1)	5.727(1)
c (Å)	5.120(1)	5.102(1)
V (Å³)	416.0(2)	415.5(1)
Measured reflections	2126	1281
ω scan angle (°)	2.5	1.5
Agreement factor for symmetric equivalent reflection intensities (%)	1.8	2.5
Reflections > $6\sigma(F_{obs})$	652	257
θ limit (°)	<40°	<30°
R (%)	4.6	2.4
R_w (%)	4.6	2.7

Note: R values are defined as follows:
$$R = (\Sigma \|F_{obs}| \cdot |F_{calc}\|)/(\Sigma |F_{obs}|)$$
$$R_w = \{[\Sigma w(|F_{obs}| \cdot |F_{calc}|)^2]/(\Sigma w|F_{obs}|^2)\}^{1/2}$$

intensities were obtained with an Enraf Nonius CAD4 single-crystal diffractometer (graphite-monochromatized MoKα X-ray radiation) using a conventional liquid N cooling device. Data for sample NCP1 were obtained at room temperature. Cell dimensions (Table 2) were refined from 24 (NCP1: 12) automatically centered reflections with $22° < \theta < 32°$ (NCP1: $11° < \theta < 34°$). The ω-θ profile plots were recorded for selected reflections, indicating strong smearing along the ω direction, which is characteristic of a high degree of crystal mosaicity. Therefore, intensities of the reflections were measured in the ω scan mode. A scan width of ca. 2.5° was used for NCP5, whereas ca. 1.5° was sufficient for NCP1 (Table 2). The final scan speed was calculated from the prescan to obtain $[\sigma(I)/I] = 0.03$. To test the quality of a subsequent absorption correction, a full sphere of reflection intensities up to $\theta = 20°$ was measured (Table 2). High-angle reflections of sample NCP5 were measured more precisely because low-angle reflections contain information on bonding electrons which are not considered in conventional refinement models (Hirshfeld, 1976). The ψ scans of five strong reflections showed significant intensity variations; thus an absorption correction had to be applied on both samples. As standard deviation, the larger σ either from averaging or counting statistics was used. Reflections of the type 0*kl* with $k \neq 2n$, *h*0*l* with $l \neq 2n$, and *hk*0 with $h + k \neq 2n$ were considered as systematically absent and were rejected. A few reflections were observed that are inconsistent with space group *Pbcn*. These were determined to be a result of multiple reflection and were omitted from the data set.

Data reduction, including background, Lorentz-polarization and absorption corrections, was performed with

the SDP program system (Enraf Nonius, 1983). Reflections allowed under *Pbcn* were employed for the refinement using the atomic coordinates of Grice et al. (1976) and the XTAL2.4 program package (Hall and Stewart, 1988). Structure factors were weighted ($w = 1/\sigma^2$), applying a $6\sigma(F_{obs})$ cutoff. Scattering factor curves for neutral atoms, as well as real and imaginary parts of anomalous dispersion correction, were applied. In the first iteration on sample NCP5, the A site was assumed to be pure Fe (simulating Fe, Mn, and Ti) and the B site pure Nb. This refinement with isotropic parameters yielded an R_w value of 8.6%. To refine the cation distribution, an interchange of Fe and Nb between the A and B sites was allowed, resulting in an R_w value of 7.3%. Subsequently, a compositional constraint according to the microprobe analyses (Table 1) was introduced, but an interchange of (Nb,Ta) and Fe on the A and B sites was still allowed. Simultaneously, the displacement parameters of the metal and O positions were refined anisotropically. Ta was assumed to share positions with Nb. Several models were calculated to determine the ratio of these two elements. This was necessary because of the strong Nb, Ta zoning determined by electron microprobe analyses. The following Nb/Ta ratios were adopted and tested: 1/0, 3/1, 1/1, and 0/1. Surprisingly, very similar site occupancies and displacement parameters were obtained independent of the prescribed Nb/Ta ratio. For partially disordered columbite, the scale factor compensates the assumed number of electrons on the metal sites (Nb/Ta ratio). Thus, an approximate Nb/Ta ratio was sufficient for the refinement. The model with Nb/Ta = 3/1 led to the best refinement (R_w = 4.6%), which is in agreement with the measured average composition. Sample NCP1 was refined using the Nb/Ta = 3/1 model with isotropic displacement parameters for O atoms, resulting in an R_w value of 2.7%. Comparison between observed and calculated structure factors indicated that an extinction correction did not have to be considered. Final difference-Fourier maps showed residual densities of ± three electrons around the B site. This is characteristic of a termination-of-series error, whose main effect is to pro-
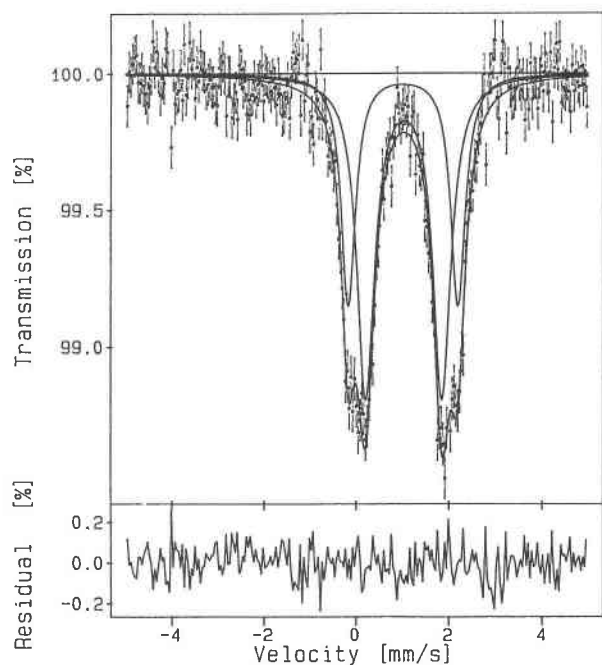
Fig. 1.　Mössbauer spectrum of columbite (NCP5) fitted with two doublets characteristic of [6]Fe^{2+}.

duce a set of approximately spherical ripples surrounding an atomic peak (Dunitz, 1979).

Measurement of [57]Fe Mössbauer data

An absorber for sample NCP5 was prepared by placing approximately 100 mg of ground material (equivalent to 8 mg Fe^{2+}/cm^2) between sheets of Al foil. The spectrum was obtained at 298 K with a nominal 50 mCi activity [57]Co in Rh source (Fig. 1). The source was also maintained at 298 K. The spectrum was recorded in a constant acceleration mode, and velocity was calibrated against Fe-metal foil; the isomer shifts are reported relative to metallic Fe (± 0.01 mm/s). A mirror image spectrum was obtained on a 512-channel multichannel analyzer, stored, and then folded. It was fitted with a least-squares program assuming Lorentzian line shapes. Experiment duration was about 1 week, and better counting statistics were prohibited by the strong absorption of γ-rays by Ta and Nb in the absorber. A previous test with only a 75-mg sample to correct for absorption yielded a significantly lower signal-to-noise ratio.

RESULTS

Table 3 summarizes the final structural parameters. Table 4 comprises a list of observed and calculated structure factors.[1] Selected interatomic distances and angles are given in Table 5.

[1] To receive a copy of Table 4, order Document AM-91-480 from the Business Office, Mineralogical Society of America, 1130 Seventeenth Street NW, Suite 330, Washington, DC 20036, U.S.A. Please remit $5.00 in advance for the microfiche.

Electron microprobe analyses yield similar average compositions for both samples NCP1 and NCP5. On the basis of six O atoms, a cation sum of three was obtained in both cases. This stoichiometry was confirmed by measuring O concentrations with the electron microprobe using a PC1 crystal and natural quartz as a standard. Back-scattered electron images showed oscillatory zones parallel to {100}. Zoning in columbite-tantalite is well known and characterized by small-scale variations in the major elements, especially in Nb and Ta (Lahti, 1987). This can also be seen in the high standard deviation of the averaged Nb_2O_5 and Ta_2O_5 concentrations of sample NCP1 (Table 1). NCP5 shows a much smaller standard deviation due to the larger compositional domain size of the measured crystal having only minor zonation. The size of a homogeneous area in a polished section depends mainly on the orientation of the zoned columbite. In general, the oscillatory zoning is similar in both samples.

Site occupancy refinement indicates a low degree of cation ordering. Figure 2 shows the ABBABB octahedral layer stacking along the **a** axis. The A site is dominated by the light transition elements (modeled by Fe) (63.8% in NCP1), whereas the B site is favored by Nb + Ta (81.9% in NCP1). Ercit's equation (Ercit, 1986) yields a cation order of 42% for sample NCP1. Cell parameters at room temperature for sample NCP5 were refined using data from a Guinier X-ray powder diffraction pattern with $FeK\alpha_1$ radiation using the program INDLSQ (Appleman and Evans, 1973) giving $a = 14.233(5)$, $b = 5.724(2)$, $c = 5.104(2)$ Å, $V = 415.8(2)$ Å^3. With Ercit's equation a similar cation order of 42% can be calculated for NCP5. These simple calculations approximate the results of the site occupancy refinement, which are 31% ordering for NCP5 and 46% for NCP1.

The site occupancies and their corresponding low standard deviations listed in Table 3 need comment. These values do not necessarily reflect the true cation distribution but are a function of a given refinement model. The model assumes the following constraints: (1) all atoms are spherical; i.e., covalently bonded electrons are not considered; (2) Nb^{5+} and Ta^{5+} show the same site preference; (3) $Nb^{5+}/Ta^{5+} = 3/1$; (4) Ti^{4+}, Fe^{2+}, and Mn^{2+} show the same site preference and are modeled as Fe; (5) (Nb,Ta)/(Fe,Mn,Ti) = 2/1. Any deviation from this model leads to slightly different site occupancies. In the case of sample NCP5, where diffraction data up to $\theta = 40°$ were measured, high-angle refinements with $\theta > 24°$ yield 42(2)% (Nb + Ta) on A compared with 46.1(5)% (Nb + Ta) when all intensity data were considered. High-angle data are not as sensitive to bonding effects (Hirshfeld, 1976). The actual Nb/Ta ratio is not very sensitive to site occupancies of disordered columbite because this ratio mainly correlates with the scale factor. A rough estimate, using varying Nb/Ta ratios, shows that site occupancies refined with the above model are correct to within 5%.

A and B sites are both coordinated by six O atoms. The Fe-dominated A site has more regular Me-O distances than the B site as demonstrated from bond-length

TABLE 3. Fractional coordinates, displacement parameters, and site occupancies of columbite from the Kings Mountain district, North Carolina

		Space group: *Pbcn* (no. 60)						
		x	y	z	B_{eq}			
A	NCP5	0	0.3328(2)	¼	1.25(2)			
	NCP1	0	0.3327(4)	¼	0.80(3)			
B	NCP5	0.16456(5)	0.17114(9)	0.7473(2)	1.057(8)			
	NCP1	0.16391(9)	0.1725(1)	0.7462(4)	0.49(1)			
O1	NCP5	0.0920(4)	0.110(1)	0.076(1)	1.15(8)			
	NCP1	0.0941(7)	0.107(1)	0.072(2)	0.7(2)			
O2	NCP5	0.4216(5)	0.117(1)	0.090(1)	1.10(7)			
	NCP1	0.4211(6)	0.117(1)	0.090(2)	0.4(2)			
O3	NCP5	0.7560(5)	0.1191(9)	0.084(1)	1.15(7)			
	NCP1	0.7577(7)	0.120(1)	0.082(2)	0.6(2)			
		U_{11}*	U_{22}	U_{33}	U_{12}	U_{13}	U_{23}	
A	NCP5	1.55(5)	1.65(5)	1.54(4)	0	0.07(6)	0	
	NCP1	0.9(1)	1.15(8)	1.05(8)	0	0.1(2)	0	
B	NCP5	1.57(3)	1.31(3)	1.14(2)	−0.03(2)	0.02(3)	0.07(6)	
	NCP1	0.49(4)	0.76(4)	0.62(4)	−0.02(5)	0.00(7)	0.1(2)	
O1	NCP5	1.6(3)	1.2(2)	1.5(2)	−0.2(2)	−0.1(2)	0.1(2)	
	NCP1	—	—	—	—	—	—	
O2	NCP5	1.5(2)	1.3(2)	1.4(2)	0.0(2)	0.1(2)	−0.4(2)	
	NCP1	—	—	—	—	—	—	
O3	NCP5	1.7(3)	1.2(2)	1.5(2)	0.2(2)	0.3(2)	−0.2(2)	
	NCP1	—	—	—	—	—	—	
		Site occupancies						
A	NCP5	46.1(5)% Nb + Ta, 53.9(5)% Fe			B	77.0(3)% Nb + Ta, 23.0(3)% Fe		
	NCP1	36.2(6)% Nb + Ta, 63.8(6)% Fe				81.9(3)% Nb + Ta, 18.1(3)% Fe		

Note: The displacement parameters are of the form $\exp(-2\pi^2 U_{11}h^2a^{*2} + U_{22}k^2b^{*2} + U_{33}l^2c^{*2} + 2U_{12}hka^*b^* + 2U_{13}hla^*c^* + 2U_{23}klb^*c^*)$. The isotropic displacement factor equivalents (B_{eq}) were calculated according to Hamilton (1959); the standard deviation of B_{eq} was estimated according to Schomaker and Marsh (1983). Data for NCP5 refined at 100 K, NCP1 at 293 K.
* $U_{ij} \times 10^2$.

distortions (BLD) calculated according to Renner and Lehmann (1986). In sample NCP5, the A octahedron has a BLD of 1.60%, whereas the B octahedron shows a higher BLD of 3.84%. The octahedral edge length distortion (ELD), also defined by Renner and Lehmann (1986), behaves conversely and is 3.14% for the B site and 3.65% for the A site.

To distinguish columbite from ixiolite in an X-ray powder diffraction pattern, supercell reflections that indicate a tripling of the *a* axis are commonly used. The columbite reflections 200 ($d = 7.21$) and 110 ($d = 5.35$) are the most important for this test. Calculation of a theoretical powder diffraction pattern of fully ordered columbite ($MnNb_2O_6$, $a = 14.413$, $b = 5.76$, $c = 5.084$ Å, Fe$K\alpha_1$ radiation, Guinier camera) with the program Lazy Pulverix (Yvon et al., 1977) yields only low intensities

TABLE 5. Selected interatomic distances (Å) and angles (°)

|	NCP5	NCP1		NCP5	NCP1
A-O1 (2×)	2.032(7)	2.070(9)	B-O1	2.005(7)	1.97(1)
A-O2 (2×)	2.085(7)	2.086(9)	B-O1	2.101(7)	2.084(9)
A-O3 (2×)	2.136(7)	2.140(9)	B-O2	1.902(7)	1.883(8)
	⟨2.084(3)⟩	⟨2.099(3)⟩	B-O3	1.968(7)	1.989(9)
			B-O3	2.057(7)	2.033(9)
O1-A-O1	102.1(3)	102.8(3)	B-O3	2.187(6)	2.197(8)
O1-A-O2 (2×)	96.3(3)	95.9(4)		⟨2.037(3)⟩	⟨2.026(3)⟩
O1-A-O2 (2×)	93.7(3)	93.9(4)			
O1-A-O2 (2×)	88.7(3)	88.2(3)	O1-B-O1	88.0(3)	88.5(4)
O2-A-O2 (2×)	81.5(3)	82.0(4)	O1-B-O2	97.9(3)	98.9(4)
O2-A-O2 (2×)	86.4(3)	86.0(4)	O1-B-O3	94.4(3)	94.6(4)
O2-A-O2	80.7(3)	80.8(3)	O1-B-O3	78.4(3)	76.9(4)
			O2-B-O1	89.8(3)	90.3(4)
			O2-B-O3	102.8(3)	103.7(3)
			O2-B-O3	95.5(3)	95.6(4)
			O3-B-O1	79.3(3)	78.3(4)
			O3-B-O1	80.5(2)	80.0(3)
			O3-B-O3	95.1(3)	94.8(4)
			O3-B-O3	87.2(3)	86.5(3)
			O3-B-O3	86.2(2)	86.5(3)
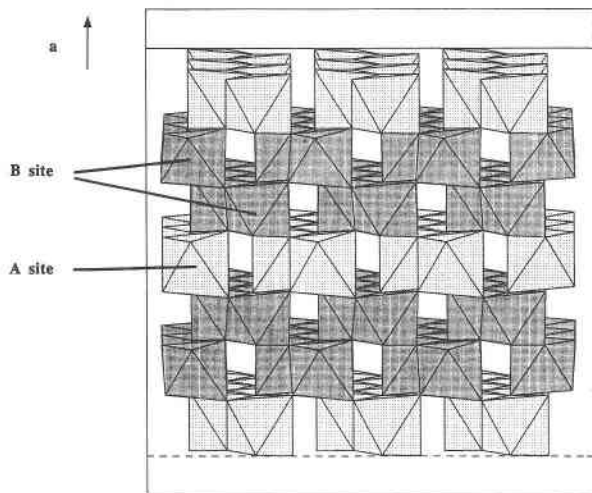
Fig. 2.   Coordination polyhedron model of columbite showing A and B octahedral chains stacked along **a**.

for the columbite supercell reflections (e.g., $I_{200} = 96$ and $I_{110} = 30$ when $I_{311} = 1000$). Actually, our first routine Guinier ($FeK\alpha_1$) powder diffraction pattern of NCP5 was first interpreted to be characteristic of ixiolite. Only a subsequent long exposure photograph made the supercell reflections visible. Thus, making a distinction between ixiolite and nearly disordered columbite only by means of their X-ray powder diffraction pattern is very doubtful; single crystal diffraction data are much more sensitive in this respect. Such methods should be used to differentiate between the two.

Within the two analytical resolution of our Mössbauer spectrum, columbite NCP5 reveals Fe in the oxidation state of Fe^{2+}. Based on the two doublet fit with isomer shifts of 1.11 and 1.13 mm/s, Fe^{2+} is considered octahedrally coordinated, which is confirmed by the results of the X-ray structure refinement. The outer doublet [quadrupole splitting 2.37(1) mm/s] is narrower (0.38 mm/s) and is interpreted as representing the less distorted octahedral site relative to the broader (0.47 mm/s) inner doublet [quadrupole splitting 1.64(2) mm/s]. Approximately 60% of Fe^{2+} is located on the site characterized by the inner doublet.

DISCUSSION

Cation-O bonding distances in the A octahedron are slightly longer in NCP1 ($\langle 2.099(3) \rangle$ Å) than in NCP5 ($\langle 2.084(3) \rangle$ Å), whereas the cation-O distances in the B octahedron are shorter for NCP1 ($\langle 2.026(3) \rangle$ Å) than for NCP5 ($\langle 2.037(3) \rangle$ Å) (Table 5). To compare the observed $\langle$A-O$\rangle$ and $\langle$B-O$\rangle$ distances with those in ordered columbite of corresponding composition, bond lengths from $FeNb_2O_6$, $MnNb_2O_6$, and $MnTa_2O_6$ end-members (Weitzel, 1976, his Table 5) were used. Linear interpolation predicts $\langle$A-O$\rangle$ distances of $\langle 2.136 \rangle$ Å for NCP5 and $\langle 2.132 \rangle$ Å for NCP1. The similar Nb/Ta ratio of 3/1 in both samples leads to a $\langle$B-O$\rangle$ distance of 2.017 Å. The

measured $\langle$A-O$\rangle$ distances are significantly shorter than the predicted ones for ordered columbite, whereas $\langle$B-O$\rangle$ distances are slightly longer. Therefore the (A,B) cation disorder is also reflected in the mean A-O and B-O distances. The larger A-O and smaller B-O distances for NCP1 relative to NCP5 are also in agreement with the slightly higher ordering in NCP1.

The bond distances of NCP5 can be modeled using known cation radii (Shannon and Prewitt, 1969, 1970) and the experimentally determined site occupancies (Table 3) to give the following: A site 46% $^{[6]}$(Nb + Ta)$^{5+}$ + 35% $^{[6]}Fe^{2+}$ + 19% $^{[6]}Mn^{2+}$ − $^{[3]}O^{2-}$ = 0.46 × 0.64 + 0.35 × 0.77 + 0.19 × 0.82 + 1.36 = 2.08 Å (observed $\langle 2.084(3) \rangle$) and B-site 77% $^{[6]}$(Nb + Ta)$^{5+}$ + 15% $^{[6]}Fe^{2+}$ + 8% $^{[6]}Mn^{2+}$ − $^{[3]}O^{2-}$ = 0.77 × 0.64 + 0.15 × 0.77 + 0.08 × 0.82 + 1.36 = 2.03 Å (observed $\langle 2.037(3) \rangle$). Good agreement between observed and calculated distances is obtained.

To check the influence of $Mn^{2+} \rightarrow Fe^{2+}$ substitutions on the cell volume, the cell parameters of $FeNb_2O_6$ ($V = 411.4$ Å^3) and $MnNb_2O_6$ ($V = 422.4$ Å^3) (Weitzel, 1976, his Table 2) were interpolated using the same model as for the cation-O distances above. A cell volume of 415 Å^3 was obtained for both samples. Nb → Ta substitution has only minor influence on the cell volume given that $MnTa_2O_6$ has $V = 421.5$ Å^3 (Weitzel, 1976). The predicted volume is in good agreement with the measured data (Table 3) indicating that the unit-cell volume is mainly a function of the Mn^{2+} for Fe^{2+} substitution and not the degree of cation order-disorder between the A and B sites.

Displacement parameters differ significantly in both samples. Surprisingly, B_{eq} values of NCP5 measured at 100 K are higher than those of NCP1 determined at room temperature. The BSE images indicate Nb, Ta variations within both crystals. In addition, ω-θ scans on intense peaks indicate strong smearing along the ω direction for sample NCP5. In contrast, sample NCP1 shows rather sharp, intense peaks. Consequently, the difference in displacement parameters must be explained by the differences in crystal mosaicity and chemical homogeneity. In this case, differences in thermal motion at different temperatures are of subordinate importance. In other words, more chemically or structurally distinct domains were averaged in the structure refinement of NCP5 compared with NCP1, and therefore positional disorder is reflected in high displacement parameters. This argument is supported by electron diffraction experiments on Kings Mountain columbite (Greis, personal communication) showing that the refined structures are averages of a variety of structural variants in the scale of a few cell dimensions. The substructure possesses $a = 4.73$, $b = 5.73$, $c = 5.12$ Å cell dimensions (ixiolite), and the most frequent superstructure is characterized by cell dimensions $3a, b, c$ (columbite). Differences in domain structures between NCP5 and NCP1 are also reflected in differences of peak shape, displacement parameters, and R values.

A direct correlation between the diffraction data and

Mössbauer results is difficult to establish because the Mössbauer effect probes exclusively the Fe sites, whereas the diffraction data provide information on the average elemental site occupation. Since the two Fe sites are only slightly different with respect to their electronic environments, they give rise to overlap in the Mössbauer spectrum. Nevertheless, a two doublet model yields a significantly better fit than a single doublet model. The latter is characterized by a very wide half-width and is thus considered unsatisfactory.

If only nearest neighbor effects are considered, the ^{57}Fe Mössbauer quadrupole splitting can be correlated with octahedral distortions. Previous studies have shown that octahedral distortions are inversely correlated with quadrupole splitting (e.g., Hafner and Ghose, 1971). In the case of the two Fe sites in neptunite, Kunz et al. (1991) showed that the octahedral edge length distortion (ELD) correlates inversely with quadrupole splitting. A similar observation can be made for columbite. The A site with the higher occupancy of light transition metals (Fe and Mn) has also a slightly higher ELD compared with the B site. The Mössbauer spectrum indicates that approximately 60% of total Fe^{2+} is localized on the more distorted site. Thus the assignment of the inner doublet to the A site seems to be justified. As in the case of neptunite (Kunz et al., 1991), it appears that the bond length distortion (BLD) is not a reliable parameter for measuring octahedral distortion. Let us consider a completely ordered ferrocolumbite $FeNb_2O_6$ or manganotantalite $MnTa_2O_6$ as reference structures (Weitzel, 1976). In these examples, the A type Fe (or Mn) octahedron exhibits regular Fe-O (or Mn-O) distances leading to BLD = 0.68% (0.94% for Mn). The edge length distortions are 4.63 and 6.35%, respectively. Nb on the B site is displaced from the center of the octahedron and has strongly different Nb-O distances leading to BLD = 6.86 and ELD = 3.25. Ta in $MnTa_2O_6$ does not display such a pronounced out-of-center displacement and has a BLD of 4.42 with ELD of 4.24. In columbite minerals with a low degree of ordering, some (Nb,Ta) is positioned on the A site and will also favor an out-of-center position within this octahedron. Because of the strong scattering power of (Nb,Ta) in the diffraction experiment, the average A and B positions are strongly influenced by these heavy cations (Nb,Ta) and not much by Fe and Mn. Thus, BLD calculated from diffraction data is largely a function of Nb and Ta and not of the lighter Fe and Mn cations. This explains why a BLD analysis fails for the assignment of the two Fe-Mössbauer doublets.

Electron microprobe and X-ray data indicate a strong chemical and structural similarity between the two investigated crystals. Columbite (sample NCP5) was clearly formed during the first stage of crystallization. During the emplacement of the pegmatite into the amphibolite and schists, second stage deformation occurred, and the brittle columbite crystals were strained and broken into small fragments (secondary stage after White, 1981). The subsequent hydrothermal activity did not significantly affect the columbite fragments. However, since only one crystal from each rock type was investigated, it remains unclear whether the higher degree of cation order in sample NCP1 is due to the later thermal influence of the hydrothermal activity or is just within the variation of order within the rock types. Thus, only one columbite-forming event must be assumed.

CONCLUSIONS

1. Columbite from the Kings Mountain district, North Carolina, shows oscillatory zoning in its chemical composition with a mean composition of $Fe_{0.65}Mn_{0.30}Ti_{0.05}Nb_{1.5}Ta_{0.5}O_6$.

2. The degree of order between the five- and two-valent charged cations in both columbite crystals is small as indicated by site occupancy refinements and mean A-O and B-O distances obtained from single-crystal X-ray structure refinements.

3. Disordered columbite can hardly by distinguished from ixiolite by its X-ray powder diffraction pattern because intensities of columbite supercell reflections are too weak.

4. Mössbauer spectroscopy reveals Fe in the oxidation state of Fe^{2+} located on two different octahedral sites.

5. The Fe^{2+} Mössbauer doublet with the stronger intensity, characteristic of the octahedral A position, has a smaller quadrupole splitting than the doublet characteristic of the octahedral B site.

6. The bond length distortion (BLD) of the A site, as obtained from the diffraction experiment, is less than the distortion of the B site, which based on a simple analysis would seem to contradict the Mössbauer doublet assignment. However, cation positions in disordered columbite are mainly influenced by the heavy elements (Nb,Ta); thus, distortion parameters (as BLD) derived from average cation positions are not reliable for the interpretation of Mössbauer results.

7. Morphological aspects, similarity in chemistry, and cation ordering suggest that in the pegmatites of the Kings Mountain district, columbite was formed only at the first stage of crystallization (sample NCP5). NCP1 is a strained and broken relict of NCP5 and not a product of secondary niobium tantalum oxide formation.

REFERENCES CITED

Appleman, D.E., and Evans, H.T. (1973) Job 9214: Indexing and least squares analyses of powder diffraction data. United States Department of Commerce, National Technical Information Service, PB 216188.

Cerný, P., and Ercit, T.S. (1989) Mineralogy of niobium and tantalum: Crystal chemical relationship, paragenetic aspects and their economic implications. In P. Möller, P. Cerný, and F. Saupé, Eds., Lanthanides, tantalum and niobium, special publication 7, p. 27–80. Springer-Verlag, New York.

Černý, P., and Turnock, A.C. (1971) Niobium-tantalum minerals from granitic pegmatites at Greer Lake, south-eastern Manitoba. Canadian Mineralogist, 10, 755–772.

Dunitz, J.D. (1979) X-ray analysis and the structure of organic molecules, 514 p. Cornell University Press, New York.

Enraf Nonius (1983) Structure determination package (SDP). Enraf Nonius, Delft, Holland.

Ercit, T.S. (1986) The simpsonite paragenesis: The crystal chemistry and geochemistry of extreme tantalum fractionation. Ph.D. thesis, University of Manitoba, Winnipeg.

Ferguson, R.B., Hawthorne, F.C., and Grice, J.D. (1976) The crystal structure of tantalite, ixiolite and wodginite from Bernic Lake, Manitoba. II Wodginite. Canadian Mineralogist, 14, 550–560.

Giese, R.F. (1975) Electrostatic energy of columbite/ixiolite. Nature, 256, 31–32.

Grice, J.D., Ferguson, R.B., and Hawthorne, F.C. (1976) The crystal structure of tantalite, ixiolite and wodginite from Bernic Lake, Manitoba. I Tantalite and ixiolite. Canadian Mineralogist, 14, 540–549.

Hafner, S.S., and Ghose, S. (1971) Iron and magnesium distribution in cummingtonites $(Fe,Mg)_7Si_8O_{22}(OH)_2$. Zeitschrift für Kristallographie, 133, 301–326.

Hall, S.R., and Stewart, J.N. (1988) XTAL2.4 User's manual. University of Western Australia, Nedlands, Australia, and University of Maryland, College Park, Maryland, U.S.A.

Hamilton, W.C. (1959) On the isotropic temperature factor equivalent to a given anisotropic temperature factor. Acta Crystallographica, 12, 609–611.

Hirshfeld, F.L. (1976) Can X-ray distinguish bonding effects from vibrational smearing? Acta Crystallographica, A32, 239–244.

Horton, J.W., and Butler, J.R. (1986) The Kings Mountain belt and spodumene pegmatite district, Cherokee and York counties, South Carolina, and Cleveland County, North Carolina. Centennial Field Guide—Southeastern section. Geological Society of America, Boulder, Colorado.

Kesler, T.L. (1961) Exploration of the Kings Mountain pegmatites. Mining and Engineering, 43, 1063–1068.

Khvostova, V.A., and Maximova, N.V. (1969) On the minerals of the tantalite-columbite group. Mineralogičeskij Sbornik State University Lvov, 23, 38–52.

Kish, S.A. (1983) A geochronology study of deformation and metamorphism in the Blue Ridge and Piedmont of Carolinas. Ph.D. thesis, University of North Carolina, Chapel Hill, North Carolina.

Komkov, A.I. (1970) Relationship between the X-ray constants of columbite and composition. Doklady Akademii Science USSR, Earth Science Section, 194, 434–436 (in Russian).

Kunz, M., Armbruster, Th., Lager, G.A., Schultz, A.J., Goyette, R.J., Lottermoser, W., and Amthauer, G. (1991) Fe, Ti ordering and octahedral distortion in acentric neptunite: Temperature dependent X-ray

and neutron structure refinements and Mössbauer spectroscopy. Physics and Chemistry of Minerals, in press.

Lahti, S.I. (1987) Zoning in columbite-tantalite crystals from the granitic pegmatites of the Eräjärvi area, southern Finland. Geochimica et Cosmochimica Acta, 51, 509–517.

Laves, F., Bayer, G., and Panagos, A. (1963) Strukturelle Beziehungen zwischen den Typen α-PbO_2, $FeWO_4$ (Wolframit) und $FeNb_2O_6$ (Columbit) und über die Polymorphie des $FeNbO_4$. Schweizerische Mineralogische und Petrographische Mitteilungen, 43, 217–234.

Nickel, E.H., Rowland, J.F., and McAdam, R.C. (1963a) Wodginite, a new tin-manganese tantalite from Wodgina, Australia and Bernic Lake, Manitoba. Canadian Mineralogist, 7, 390–402.

——— (1963b) Ixiolite—a columbite substructure. American Mineralogist, 48, 961–979.

Nordenskiöld, A.E. (1857) Beitrag zu Finnlands Mineralogie. Annalen der Physik und Chemie, 4th serie, 11, 625–634.

Renner, B., and Lehmann, G. (1986) Correlation of angular and bond length distortion in TO_4 units in crystals. Zeitschrift für Kristallographie, 175, 43–59.

Schomaker, V., and Marsh, R.E. (1983) On evaluating the standard deviation of U_{eq}. Acta Crystallographica, A39, 819–820.

Shannon, R.D., and Prewitt, C.T. (1969) Effective ionic radii in oxides and fluorides. Acta Crystallographica, B25, 925–946.

——— (1970) Revised values of effective ionic radii. Acta Crystallographica, B26, 1046–1048.

Spanjers, R.P. (1988) FMC-LITHCO Hallman-beam spodumene pegmatite mine. South Carolina Geological Survey, 24th forum on the geology on industrial minerals, 25–29.

Sturdivant, J.H. (1930) The crystal structure of columbite. Zeitschrift für Kristallographie, 75, 88–108.

Turnock, A.C. (1966) Synthetic wodginite, tapiolite and tantalite. Canadian Mineralogist, 8, 461–470.

Weitzel, H. (1976) Kristallstrukturverfeinerungen von Wolframiten und Columbiten. Zeitschrift für Kristallographie, 144, 238–258.

White, J.S. (1981) Mineralogy of the Foote mine, Kings Mountain, North Carolina. In J.W. Horton, J.R. Butler, and D.J. Milton, Eds., Geological investigations of the Kings Mountain belt and adjacent areas in the Carolinas, p. 39–48. Carolina Geological Society Field Trip Guidebook 1981, South Carolina Geological Survey, Columbia, South Carolina.

Wise, M.A., Turnock, A.C., and Černý, P. (1985) Improved unit cell dimensions for ordered columbite-tantalite end members. Neues Jahrbuch für Mineralogie Monatshefte, 8, 372–378.

Yvon, K., Jeitschko, W., and Parthe, E. (1977) Lazy Pulverix. A program to calculate theoretical X-ray and neutron diffraction powder patterns. Journal of Applied Crystallography, 10, 73.